Numerical Heat Transfer, Part A, 35:859–873, 1999

1040–7782/99 $12.00 + .00

NONEQUILIBRIUM HEATING IN METAL FILMS: AN ANALYTICAL AND NUMERICAL ANALYSIS

Andrew N. Smith, John L. Hostetler, and Pamela M. Norris
Department of Mechanical and Aerospace Engineering, University of Virginia, Charlottesville, Virginia 22903, USA

Ultrashort pulsed laser heating of metals at room temperature is commonly studied using the parabolic two step (PTS) model. An analytical solution of the PTS is presented and compared to numerical results. The analytical solution assumes constant thermophysical properties, which is appropriate for applications such as nondestructive testing using low laser fluences. The assumption of constant thermophysical properties is discussed, and appropriate regimes are established. Numerical and analytical solutions of the PTS model are compared to experimental data in order to demonstrate the utility of these solutions for determining the thermal diffusivity of thin films.

INTRODUCTION

Measurement of the thermophysical properties of thin films has become a matter of extreme importance to the microelectronics industry. Many of the properties of thin film materials vary in some manner from the corresponding bulk material. For example, the deposition technique and substrate can directly affect the grain structure of the film, interfacial properties, surface roughness, density, and subsequently, the thermophysical properties. Certain transport properties, such as thermal conductivity, can be affected simply due to the size of the film [1, 2]. This reduction in thermal diffusivity has been experimentally measured using a transient thermoreflectance technique [3, 4]. This technique utilizes an intense heating beam, which creates a thermal response at the surface of a metallic material. This transient response is observed by monitoring the small changes in reflectivity of the sample surface using a weaker probe beam. The change in reflectivity of the metal is then related to the change in temperature. Thermal excitation of thin films requires the use of ultrashort laser pulses in order to resolve transport within the film prior to the effects of the substrate. There are many advantages to using femtosecond pulse durations, which provide high temporal resolution measurements. However, the drawback is that ultrashort laser pulses induce nonequilibrium heating, resulting in a more complicated model for the heat transfer [4–7].

The appropriate model for describing heat transfer during the nonequilibrium heating is the parabolic two step (PTS) model, which is represented by a pair of coupled nonlinear partial differential equations. The coupling parameter, called

Received 29 October 1998; accepted 4 January 1999.
The authors are grateful to the National Science Foundation and the National Defense Science and Engineering Graduate Fellowship program for their financial support.
Address correspondence to Andrew N. Smith, Department of Mechanical and Aerospace Engineering, Thornton Hall, University of Virginia, Charlottesville, VA 22903-2442, USA.

NOMENCLATURE

A	Fourier coefficients
B	constant coefficients
C	heat capacity, J/(m^3 K)
C_e	electron heat capacity constant, J/(m^3 K^2)
C_r	ratio of electron to lattice heat capacity
d	radiation penetration depth, m
D	nondimensional parameter, Eq. (43)
G	electron-phonon coupling factor, W/(m^3 K)
h	temporal dependent variable
J	laser fluence, J/m^2
k	electron thermal conductivity, W/(m K)
L	film thickness, m
m	coefficient defined by Eq. (22)
n	index for the eigenvalues
N	nondimensional pulse width
Q	laser heating source, W/m^3
Q_d	discrete laser heating source
R	reflectivity
S	nondimensional laser fluence
t	time, s
t_p	laser pulse duration, s
T	temperature, K
x	direction normal to surface, m
α	thermal diffusivity, m^2/s
β	coefficient defined by Eq. (34)
δ	delta function
η	nondimensional distance normal to surface
θ	nondimensional temperature
λ	eigenvalues
μ	coefficient defined by Eq. (9)
τ	nondimensional time
τ_c	thermalization time, s
υ	coefficient defined by Eq. (8)
ϕ	coefficient defined by Eq. (35)
Φ	spatial dependent variable
ψ	coefficient defined by Eq. (32)

Subscripts

e	electron
eff	effective
eq	equilibrium
i	spatial node
l	lattice
n	time increment
0	initial

the electron-phonon coupling factor, has been experimentally measured for several metals [8, 9]. The electron-phonon coupling factor is assumed to be constant near room temperature [10]. The electron heat capacity and the thermal conductivity are dependent on the electron and lattice temperatures. These temperature dependent properties cause the partial differential equations to be nonlinear. While these equations can be solved numerically with reasonable accuracy, analytical solutions are often attempted.

The most common assumption made when solving the PTS equations analytically is that the thermophysical properties are constant. This assumption is only valid for low values of the laser fluence. A regime map developed in this investigation shows when the temperature dependent properties must be taken into account. This assumption makes the equations linear and allows for solutions using Green's functions [11] and Laplace transforms [12]. These solutions still require numerical integrals due to the Gaussian laser source term. Hays-Stang and Haji-Sheikh [11] derive a Green's function with a solution assuming an instantaneous surface source and employing Fourier series. There have also been solutions concentrating on the absorption and diffusion of energy by the electron system prior to any coupling with the lattice [13, 14]. These solutions account for the temperature dependent properties but are only valid within the first few picoseconds after intense heating periods.

Assuming an instantaneous source and constant thermophysical properties, an analytical solution will be presented using a Fourier cosine series. The exponential decay of the source within the material will be taken into account. It will be shown that this solution is sufficient for comparison to experimental data when the pulse duration is less than the thermalization time and when the laser fluence values are low. This solution captures the essential effects of the nonequilibrium heating on the lattice and the electron systems once they have reached equilibrium. However, since the temperature dependence of the electron heat capacity is ignored, the solution will never sufficiently represent the electron temperature during the nonequilibrium period.

THEORY

The existence of non-Fourier heat conduction has been experimentally observed at cryogenic temperatures and during ultrashort laser heating of metals [15]. It has been theorized that the radiant energy is first absorbed by the electrons and then transferred to the lattice [5]. This exchange of energy occurs within the first few picoseconds and must be considered when the pulse duration is of comparable magnitude. In 1974, Anisimov presented a two-temperature model, later called the PTS, which assumes that the lattice and electrons can be described by separate temperatures, T_l and T_e [6]:

$$C_e(T_e)\frac{\partial T_e}{\partial t} = \frac{\partial}{\partial x}\left(k_e(T_e, T_l)\frac{\partial T_e}{\partial x}\right) - G(T_e - T_l) + Q \tag{1}$$

$$C_l\frac{\partial T_l}{\partial t} = G(T_e - T_l) \tag{2}$$

The electron-phonon coupling factor G is a material property that represents the rate of energy transfer between the electrons and the lattice. The heat capacity of the electrons and the lattice, C_e and C_l, and the thermal conductivity of the electrons, k_e, are also material properties. While all these material properties have some temperature dependence, the electron heat capacity is a strong function of the electron temperature:

$$C_e = C_e' T_e \tag{3}$$

The values of C_e' are given by Kittel [16]. The electron-phonon coupling factor and the lattice heat capacity are assumed to be constant. The temperature dependence of the thermal conductivity during the nonequilibrium heating can be approximated as [13]

$$k_e(T_e, T_l) = k_{\text{eq}}(T_0)\frac{T_e}{T_l} \tag{4}$$

where k_{eq} is the equilibrium electron thermal conductivity measured at room temperature.

The laser source term Q in Eq. (1) has an exponential decay in space to account for absorption in a nontransparent media, and a Gaussian shape in time, which is a reasonable approximation of the pulse shape [7]:

$$Q = 0.94\frac{(1-R)}{t_p d}J\exp\left[-\frac{x}{d} - 2.77\left(\frac{t}{t_p}\right)^2\right] \tag{5}$$

The reflectivity R and the penetration depth d are material properties, while the fluence J and the pulse width t_p are parameters of the incident laser pulse. This source term neglects any interaction with the substrate; therefore the film must be thicker than the radiation penetration depth to ensure that the radiant energy does not reach the substrate.

ANALYTICAL SOLUTION

Assuming constant thermophysical properties, T_e can be eliminated from Eqs. (1) and (2). The result is the following equation for the lattice temperature of the PTS model [11]. This second-order partial differential equation is similar to the Jeffreys heat equation, which is still diffusive and therefore parabolic [17]:

$$C\frac{\partial T_l}{\partial t} + \upsilon\frac{\partial^2 T_l}{\partial t^2} = k\frac{\partial^2 T_l}{\partial x^2} + \mu k\frac{\partial^2}{\partial x^2}\left(\frac{\partial T_l}{\partial t}\right) + Q \tag{6}$$

where

$$C = C_e + C_l \tag{7}$$

$$\upsilon = \frac{C_e C_l}{G} \tag{8}$$

$$\mu = \frac{C_l}{G} \tag{9}$$

In Eq. (6), it is easily observed that as G approaches infinity, υ and μ diminish and the PTS reduces to the standard Fourier heat diffusion equation. This makes physical sense because as G goes to infinity there is instantaneous coupling of energy between the electrons and the lattice.

The thermalization time is generally defined by the time required for the electron lattice temperature difference to fall by a factor of $1/e$, assuming an initial uniform electron temperature that is different from an initial uniform lattice temperature. The common derivation, which assumes constant thermophysical

properties, yields the following equation [7]:

$$\tau_c = \left(\frac{C_e C_l}{C_e + C_l}\right)\frac{1}{G} \cong \frac{C_e}{G} \tag{10}$$

where G is the electron-phonon coupling factor. The simplification is possible, since the electron heat capacity C_e is at least an order of magnitude less than the lattice heat capacity C_l at room temperature [16].

Diffusion of energy through the lattice occurs on the picosecond timescale. Therefore, if the pulse width of the laser is of the order of or less than the thermalization time, the pulse duration is negligible on the timescale of interest. In this case the laser pulse can be approximated by a delta function in time with reasonable accuracy. To ensure conservation of energy, the Gaussian term is integrated over time and multiplied by a delta function. The resulting source term is expressed by

$$Q = (1 - R)\frac{J}{d}\exp\left(-\frac{x}{d}\right)\delta(t) \tag{11}$$

where $\delta(t)$ represents a delta function in time. The energy from the source term is instantaneously deposited and absorbed by the electrons at time $t = 0$. Therefore the diffusion and the electron-phonon coupling terms can be neglected during the deposition of energy, and the equation is integrated to find the electron temperature distribution just after the arrival of the heating pulse:

$$\int_{0^-}^{0^+} C_e \frac{\partial T_e}{\partial t}\, dt = \int_{0^-}^{0^+} (1 - R)\frac{J}{d}\exp\left(-\frac{x}{d}\right)\delta(t)\, dt \tag{12}$$

$$T_e(x, 0^+) = \frac{(1 - R)J}{C_e d}\exp\left(-\frac{x}{d}\right) \tag{13}$$

Using Eq. (2) to relate $T_e(x, t)$ and $\partial T_l/\partial t(x, t)$ results in the following initial conditions:

$$T_l(x, 0^+) = T_l(x, 0^-) = 0 \tag{14}$$

$$\frac{\partial T_l}{\partial t}(x, 0^+) = \frac{(1 - R)J}{\upsilon d}\exp\left(-\frac{x}{d}\right) \tag{15}$$

The substrate is assumed to be an insulating material, and convection and radiation from the surface are neglected owing to the small temperature rise and the timescale of interest. Therefore homogeneous boundary conditions of the second kind are applied for this solution:

$$\frac{\partial T_l}{\partial x}(0, t) = \frac{\partial T_l}{\partial x}(L, t) = 0 \tag{16}$$

where L is the film thickness. Applying these initial conditions and insulated boundary conditions, the governing partial differential equation can then be solved using the method of separation of variables. The result is two ordinary differential equations, one with spatial dependence and the other with temporal dependence:

$$\frac{d^2\Phi}{dx^2} + \lambda\Phi = 0 \tag{17}$$

$$\upsilon\frac{d^2h}{dt^2} + (C + \lambda\mu k)\frac{dh}{dt} + \lambda kh = 0 \tag{18}$$

Applying the boundary conditions and solving for the x dependence and the eigenvalues yields

$$\Phi(x) = A_0 + \sum_{j=1}^{\infty} A_j \cos\left(\frac{j\pi x}{L}\right) \tag{19}$$

$$\lambda_j = \left(\frac{j\pi}{L}\right)^2 \tag{20}$$

The solution to the time dependent equation is

$$h(t) = B_1 e^{m_1 t} + B_2 e^{m_2 t} \tag{21}$$

where

$$m_{1,2} = \frac{-(C + \lambda_j\mu k) \pm \sqrt{(C + \lambda_j\mu k)^2 - 4\lambda_j\upsilon k}}{2\upsilon} \tag{22}$$

Applying the first initial condition yields

$$h(t) = B_1(e^{m_1 t} - e^{m_2 t}) \tag{23}$$

Therefore the general solution for the lattice and electron temperature can be written as

$$T_l(x, t) = A_0\left(1 - e - \frac{ct}{\upsilon}\right) + \sum_{j=1}^{\infty} A_j(e^{m_1 t} - e^{m_2 t})\cos\frac{j\pi x}{L} \tag{24}$$

$$T_e(x, t) = \frac{C_l}{G}\frac{\partial T_l(x, t)}{\partial t} + T_l(x, t) \tag{25}$$

Using the second initial condition, the coefficients can be found:

$$A_0 = \frac{(1 - R)J}{LC}(1 - e^{-L/d}) \tag{26}$$

$$A_j = \frac{2(1 - R)J}{(m_1 - m_2)L\upsilon}\left[\frac{(1 - e^{-L/d}\cos j\pi)}{1 + \left(\frac{dj\pi}{L}\right)^2}\right] \tag{27}$$

The analytical solution typically requires ~ 50 terms in the summation to converge to an answer with 0.1% error, thus still requiring some computational effort.

NUMERICAL SOLUTION

Finite differencing methods can be employed to solve this system of equations and determine approximate temperatures at discrete time intervals and nodal points. Equations (1) and (2) are solved numerically using the Crank-Nicolson method. To provide accuracy, difference approximations are developed at the midpoint of the time increment. To accomplish this, the time derivative can be approximated by

$$\frac{\partial T}{\partial t} = \frac{(T_{i,n+1} - T_{i,n})}{\Delta t} \tag{28}$$

where n represents a time increment and i represents a spatial node. A second derivative in space is evaluated by an average of two central difference quotients, one evaluated at the present time increment and the other at the future time increment $n+1$:

$$\frac{\partial^2 T}{\partial x^2} = \frac{1}{2}\left[\frac{(T_{i+1,n+1} - 2T_{i,n+1} + T_{i-1,n+1})}{\Delta x^2} + \frac{(T_{i+1,n} - 2T_{i,n} + T_{i-1,n})}{\Delta x^2}\right] \tag{29}$$

Applying these differencing equations to Eqs. (1) and (2) and evaluating the electron heat capacity at $T_{e,i,n}$ results in the following equations.

Electron temperature

$$\begin{aligned} -\psi_i T_{e\,i+1,n+1} + [T_{e\,i,n} + (\psi_i + \psi_{i-1}) + \phi] T_{e\,i,n+1} + -\psi_{i-1} T_{e\,i-1,n+1} \\ = \psi_i T_{e\,i+1,n} - (\psi_i + \psi_{i-1}) T_{e\,i,n} + \psi_{i-1} T_{e\,i-1,n} \\ + 2\phi T_{l\,i,n} - \phi T_{e\,i,n} + T_{e\,i,n}^2 + Q_d \end{aligned} \tag{30}$$

Lattice temperature

$$T_{l\,i,n+1} = \frac{\beta}{1+\beta}(T_{e\,i,n+1} + T_{e\,i,n} - T_{l\,i,n}) + \frac{1}{1+\beta} T_{l\,i,n} \tag{31}$$

where

$$\psi_i = \frac{k_{\text{eff},i}\Delta t}{2C_e \Delta x^2} \tag{32}$$

$$k_{\text{eff},i} = \frac{2k_i k_{i+1}}{k_i + k_{i+1}} \tag{33}$$

$$\beta = \frac{G\Delta t}{2C_l} \tag{34}$$

$$\phi = \frac{G\Delta t}{2C_e'(1+\beta)} \tag{35}$$

and

$$Q_d = \frac{0.94(1-R)J\Delta t}{C_e' t_p d} \exp\left[-\left(\frac{i\Delta x}{d}\right) - 2.77\left(\frac{n\Delta t}{t_p}\right)^2\right] \tag{36}$$

Evaluating the temperature at each node and applying the boundary conditions results in a linear system of equations. The system can be arranged in matrix form, where the coefficient matrix is a tridiagonal matrix representing the coefficients of the unknown temperatures, $T_{i,n+1}$, and solved by LU decomposition.

The numerical solution reached the desired accuracy of 0.1% with a grid spacing of 0.5 nm and a time increment of ~ 0.01 ps, depending on the pulse duration. The results were stable using the Crank-Nicolson algorithm within the range of realistic parameters. The total energy contained in the system was calculated at each time increment and compared to the energy generated by the source term. The total energy was always within 0.01% of the expected value.

NONDIMENSIONAL EQUATIONS

The assumption of constant thermophysical properties is only reasonable when the fluence value is low; therefore it is necessary to define a regime where this assumption is reasonable. In order to compare the solutions of the PTS using different expressions for the thermophysical properties, the PTS is expressed in a nondimensional form appropriate for each set of assumptions. Using the following nondimensional variables,

$$\theta_e = \frac{T_e}{T_0} \tag{37}$$

$$\theta_l = \frac{T_l}{T_0} \tag{38}$$

$$\eta = \frac{x}{d} \tag{39}$$

$$\tau = \frac{t}{t_p} \tag{40}$$

the PTS can be expressed in nondimensional form using Eqs. (3) and (4) for the electron heat capacity and the thermal conductivity:

$$\theta_e \frac{\partial \theta_e}{\partial \tau} = DN \frac{\partial}{\partial \eta}\left(\frac{\theta_e}{\theta_l}\frac{\partial \theta_e}{\partial \eta}\right) - N(\theta_e - \theta_l) + 0.94 S \exp(-\eta - 2.77\tau^2) \tag{41}$$

$$\frac{\partial \theta_l}{\partial \tau} = NC_r(\theta_e - \theta_l) \tag{42}$$

with the following nondimensional parameters:

$$D = \frac{k_e}{Gd^2} \tag{43}$$

$$N = \frac{t_p}{\tau_c} \tag{44}$$

$$S = \frac{(1-R)J}{C_e T_0 d} \tag{45}$$

$$C_r = \frac{C_e}{C_l} \tag{46}$$

Assuming constant thermophysical properties results in the following equation for the electron temperature.

$$\frac{\partial \theta_e}{\partial \tau} = DN \frac{\partial^2 \theta_e}{\partial \eta^2} - N(\theta_e - \theta_l) + 0.94 S \exp(-\eta - 2.77\tau^2) \tag{47}$$

The lattice equation, Eq. (42), and the nondimensional parameters remain the same. Finally, assuming an instantaneous source and using the thermalization time as the characteristic time, $\tau = t/\tau_c$, the following equations result:

$$\frac{\partial \theta_e}{\partial \tau} = D \frac{\partial^2 \theta_e}{\partial \eta^2} - (\theta_e - \theta_l) + S \exp(-\eta)\delta(\tau) \tag{48}$$

$$\frac{\partial \theta_l}{\partial \tau} = C_r(\theta_e - \theta_l) \tag{49}$$

The nondimensional form of the PTS with an instantaneous source, Eqs. (48) and (49), has one less parameter than with a finite pulse, Eqs. (42) and (47). This result is expected, since the original differential equation is dependent on one less parameter, the pulse duration. The nondimensional parameter D can range from 0.1 to 100 and represents the effects of diffusion versus coupling within the penetration depth. The ratio of the electron to lattice heat capacity at room temperature, C_r, varies only slightly between 0.005 and 0.015. The ratio of the

pulse width to the thermalization time, N, can be any value greater than ~ 0.01. Finally, the parameter S is the ratio of the absorbed fluence to the amount of thermal energy stored by electrons within the penetration depth. This parameter can be almost any value, limited only by laser power. Qiu and Tien discuss two additional parameters that are required to fully describe the nondimensional solution [7]. These parameters are the nondimensional length and a diffusion term based on the length, which accounts for the influence of the rear boundary on the solution. The purpose of the analytical solution developed here is to determine the thermal diffusivity prior to the influence of the substrate material. Therefore the assumption is made that the film is thick enough to neglect the influence of the rear boundary on the timescale of interest.

ANALYTICAL VERSUS NUMERICAL SOLUTION

The analytical and numerical solutions are compared in the next section for the case of moderate fluence values, $S = 7$, and where the effects of diffusion and coupling are balanced during the nonequilibrium period, $D = 1$. The effects of the pulse duration are examined by varying N between 0.1, representative of ultrashort pulses ($\sim$ 6–80 fs), and $N = 1$, representative of longer pulses ($\sim$ 100–800 fs). Figure 1 shows the analytical solution compared to numerical results assuming either constant or temperature dependent properties with $N = 0.1$. For this case the pulse duration is short relative to the thermalization time, and the analytical solution gives reasonable results as compared to the numerical solution assuming constant thermophysical properties. However, since the heat capacity is linearly related to temperature, the electron temperature is actually much lower. For this reason, the analytical solution will never give accurate results during the nonequilibrium period.

The same analysis was performed with $N = 1$. Figure 2 shows that when the pulse duration is of the order of the thermalization time, the heating time has a significant effect on the electron response. However, despite the influence of the pulse duration, the nonequilibrium effects are similar, and the solutions converge after a few picoseconds.

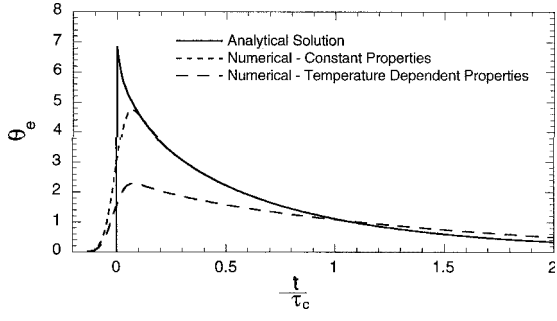

Figure 1. Comparison of the analytical and numerical solutions during the nonequilibrium period assuming a moderate laser fluence, $S = 7$, balanced diffusion and coupling effects, $D = 1$, and ultrashort pulse durations, $N = 0.1$.

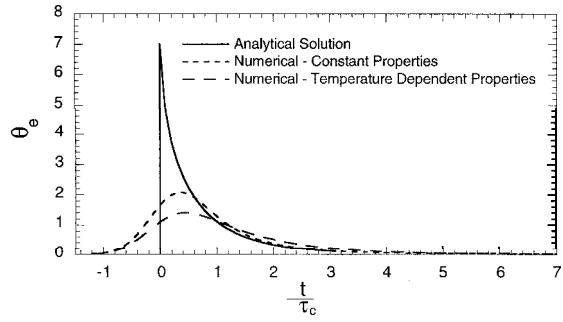

Figure 2. Comparison of the analytical and numerical solutions during the nonequilibrium period assuming a moderate laser fluence, $S = 7$, balanced diffusion and coupling effects, $D = 1$, and a pulse duration of the order of the thermalization time, $N = 1$.

In a later section it will be shown that for low laser fluence values, $S < 7$, the assumption of constant thermophysical properties is reasonable. Figure 3 shows a comparison of the analytical and numerical solutions assuming constant thermophysical properties with different values of N. The effects of a finite pulse duration on the electron response after the nonequilibrium period for values of $N < 1$ are minimal.

If the assumption of constant thermophysical properties were always reasonable, the analytical solution would be robust even for pulse durations on the order of the thermalization time. In reality, the assumption of constant thermophysical properties is only reasonable at rather low fluences. Figure 4 shows that the temperature dependence of the thermophysical properties has an effect on the electron temperature response even after the electrons and lattice have reached local thermal equilibrium.

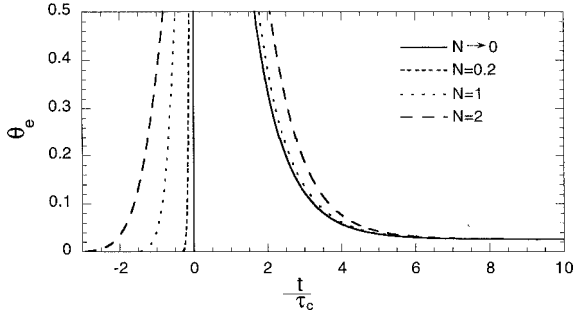

Figure 3. Influence of pulse duration on the electron response once the electrons and lattice have thermalized. These calculations assume a moderate laser fluence, $S = 7$, and balanced diffusion and coupling effects, $D = 1$.

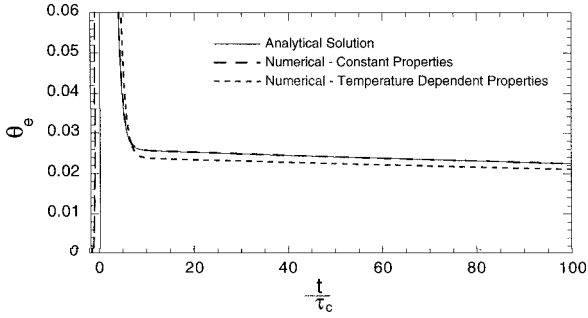

Figure 4. Influence of pulse duration on the electron response once the electrons and lattice have thermalized. These calculations assume a moderate laser fluence, $S = 7$, balanced diffusion and coupling effects, $D = 1$, and a pulse duration of the order of the thermalization time, $N = 1$.

TEMPERATURE DEPENDENT PROPERTIES

In order to establish the regime in which constant thermophysical properties can be assumed, the numerical solution with temperature dependent properties was compared to a numerical solution with constant properties after the nonequilibrium period. A critical value of the laser fluence was determined, which resulted in an error of 10% between the electron temperatures predicted by each solution. The results are shown in Figure 5. Notice that as N becomes smaller the curves converge, which is consistent with the assumption of an instantaneous solution where the solution is less dependent on the pulse duration and more on the thermalization time. In addition, as N increases, the range of values for S over which constant properties can be assumed increases. This is reasonable, since as N increases, the relative amount of nonequilibrium decreases until the standard heat diffusion equation or parabolic one step model is appropriate. In the parabolic one

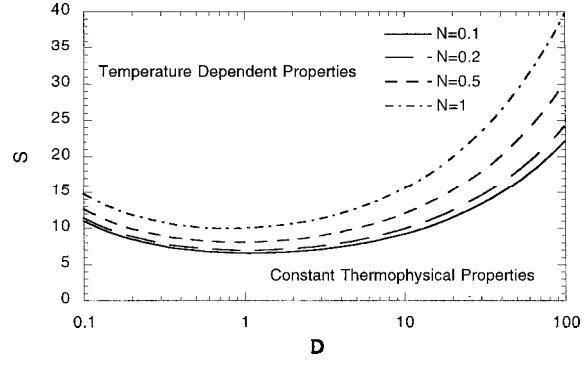

Figure 5. Regime map delineating when the assumption of constant thermophysical properties is appropriate based on a 10% error.

step model the electron and lattice are in equilibrium. This negates the temperature dependence of the thermal conductivity. In addition, the lattice heat capacity dominates, thereby reducing the effect of the electron heat capacity.

EXPERIMENTAL RESULTS

The application of a transient thermoreflectance technique with a femtosecond laser enables highly localized measurements of the thermophysical and mechanical properties of thin film materials. The local thermal diffusivity normal to the surface can be determined from a curve fit of the experimental data. The method relies on an intense heating/pump beam to generate a transient thermal response. Since the reflectivity of metals is linearly related to small changes in temperature, a weak probing beam is used for detection. The details of the experimental setup are described by Hostetler et al. [4].

Figure 6 shows the results of a scan, using a 200 fs full width at half maximum (FWHM) pulse, taken on a 365 nm tungsten film evaporated on silicon. The experimental data were compared to the electron temperature response calculated with analytical and numerical solutions of the PTS model. A least squares fit was performed to determine the only free parameter, thermal diffusivity. Only the data from 30 to 250 ps were utilized, since after 250 ps the influence of the substrate has reached the surface, and before 30 ps there is an influence due to strain induced by thermal expansion. The thermal expansion also generates an acoustic pulse that travels through the film and reflects at the film/substrate interface. This effect of the acoustic pulse first appears at the surface $\sim$ 120 ps later and lasts about 30 ps; therefore the data from 120 to 150 ps were also excluded from the curve-fitting routine.

Figure 5 indicates that the assumption of constant thermophysical properties is reasonable for these experimental conditions where $N = 1.3$, $D = 1.3$, and $S = 7.5$; however, this assumption will introduce some error between the analytical and numerical models. The value of thermal diffusivity found using the analytical solution was 26×10^{-6} m^2/s. The numerical solution, taking into account the temperature dependence of the thermophysical properties and the Gaussian pulse

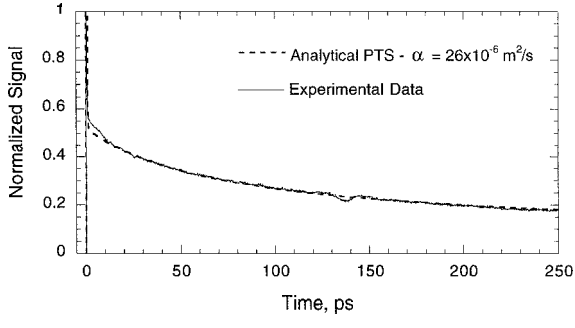

Figure 6. Experimental results for a 365 nm tungsten film shown with the analytical solution using a curve-fit of thermal diffusivity, $\alpha = 26 \times 10^{-6}$ m^2/s.

duration of 200 fs FWHM, yielded a curve-fit thermal diffusivity of 30×10^{-6} m^2/s. The numerical result was about 15% higher than the analytical solution. However, the analytical solution required significantly less computational effort for two reasons. First, the summation requires less time than a single time increment of the numerical solution. Second, the analytical solution is only evaluated at the times corresponding to data points, while the numerical solution requires a time step much less than the time between data points.

CONCLUSIONS

Numerical and analytical solutions to the parabolic two step model have been presented. The analytical solution assumes constant thermophysical properties and an instantaneous heating source. This solution can be used to curve fit for the thermal diffusivity of thin films when the pulse width of the laser is less than the thermalization time of the material and when constant thermophysical properties can be assumed. A regime map has been presented that clearly shows when temperature dependent properties must be taken into account. This regime map is based on three nondimensional parameters when the pulse duration is of the order of the characteristic time; however, the curves converge when the pulse duration is less than the thermalization time.

The analytical and numerical solutions were used to curve fit experimental data taken on a 365 nm tungsten film in order to determine the thermal diffusivity. The difference in the results was $\sim 15\%$, which is within the current accuracy of transient thermoreflectance techniques. The analytical solution requires significantly less computational effort. This increases the feasibility of using the pump probe technique as an in situ sensor, especially for situations where monitoring variations in thermophysical properties is as important as the absolute measurement.

REFERENCES

1. M. I. Flik, B. I. Choi, and K. E. Goodson, Heat Transfer Regimes in Microstructures, *J. Heat Transfer*, vol. 114, pp. 666–674, 1995.
2. T. Q. Qiu and C.-L. Tien, Size Effects an Nonequilibrium Laser Heating of Metal Films, *J. Heat Transfer*, vol. 115, pp. 842–847, 1993.
3. C. A. Paddock and G. L. Eesley, Transient Thermoreflectance from Thin Metal Films, *J. Appl. Phys.*, vol. 60, pp. 285–290, 1986.
4. J. L. Hostetler, A. N. Smith, and P. M. Norris, Thin Film Thermal Conductivity and Thickness Measurements Using Picosecond Ultrasonics, *Microscale Thermophys. Eng.*, vol. 1, pp. 237–244, 1997.
5 M. I. Kaganov, I. M. Lifshitz, and L. V. Tanatarov, Relaxation Between Electrons and the Crystalline Lattice, *Sov. Phys. JETP*, vol. 4, pp. 173–178, 1957.
6. S. I. Anisimov, B. L. Kapeliovich, and T. L. Perel'man, Electron Emission from Metal Surfaces Exposed to Ultrashort Laser Pulses, *Sov. Phys. JETP*, vol. 39, pp. 375–377, 1974.
7. T. Q. Qiu and C.-L. Tien, Short-Pulse Laser Heating on Metals, *Int. J. Heat Mass Transfer*, vol. 35, pp. 719–725, 1992.

8. S. D. Brorson, A. Kazeroonian, J. S. Moodera, D. W. Face, T. K. Cheng, E. P. Ippen, M. S. Dresselhaus, and G. Dresselhaus, Femtosecond Room-Temperature Measurement of the Electron-Phonon Coupling Constant λ in Metallic Superconductors, *Phys. Rev. Lett.*, vol. 64, pp. 2172–2175, 1990.
9. H. E. Elsayed-Ali, T. B. Norris, M. A. Pessot, and G. A. Mourou, Time-Resolved Observation of Electron-Phonon Relaxation in Copper, *Phys. Rev. Lett.*, vol. 58, pp. 1212–1215, 1987.
10. P. B. Allen, Theory of Thermal Relaxation of Electrons in Metals, *Phys. Rev. Lett.*, vol. 59, pp. 1460–1463, 1987.
11. K. J. Hays-Stang and A. Haji-Sheikh, An Analytical Solution of Heat Transfer in Thin Films, ASME HTD-vol. 293, pp. 1–7, 1994.
12. D. Y. Tzou, *Macro- to Microscale Heat Transfer*, pp. 123–126, Taylor & Francis, Washington, D.C., 1997.
13. N. K. Sherman, F. Brunel, P. B. Corkum, and F. A. Hegmann, Transient Response of Metals to Ultrashort Pulse Excitation, *Opt. Eng.*, vol. 28, pp. 1114–1121, 1989.
14. A. P. Kanavin, I. V. Smetanin, V. A. Isakov, and Yu. V. Afanasiev, Heat Transport in Metals Irradiated by Ultrashort Laser Pulses, *Phys. Rev. B*, vol. 57, pp. 14698–14703, 1998.
15. S. D. Brorson, J. G. Fujimoto, and E. P. Ippen, Femtosecond Electronic Heat-Transport Dynamics in Thin Gold Films, *Phys. Rev. Lett.*, vol. 59, pp. 1962–1965, 1987.
16. C. Kittel, *Introduction to Solid State Physics*, 7th ed., John Wiley, New York, 1996.
17. D. D. Joseph and L. Preziosi, Heat Waves, *Rev. Mod. Phys.*, vol. 61, pp. 41–73, 1989.